Generation and noise analysis of a wide-band optical frequency comb based on recirculating frequency shifter

Ying Yu (于 瀛), Cheng Lei (雷 诚), Minghua Chen (陈明华)*, Hongwei Chen (陈宏伟), Sigang Yang (杨四刚), and Shizhong Xie (谢世钟)

Tsinghua National Laboratory for Information Science and Technology (TNList)
Department of Electronic Engineering, Tsinghua University, Beijing 100084, China
**Corresponding author: chenmh@mail.tsinghua.edu.cn*

Received April 9, 2014; accepted June 18, 2014; posted online September 25, 2014

By optimizing the gain configuration and length of the loop, a 90-tone optical frequency comb (OFC) is successfully generated based on recirculating frequency shifter structure. The peak-to-peak power fluctuation of the 90-tone OFC is 4.26 dB and the tone-to-noise ratio is higher than 19.17 dB. To further analyze the noise accumulation feature of the tones when travelling around the loop, linewidth of the tones is measured by delayed self-heterodyne interferometer structure. The result shows the linewidth of the tones deteriorates little during the recirculating process, indicating that the generated OFC is an ideal multi-wavelength source for high-speed communication systems.

OCIS codes: 060.0060, 060.2380, 060.4510.
doi: 10.3788/COL201412.100601.

With the sharp increase in the demand of transmission capacity, communication systems with Tb/s bitrate and beyond based on wavelength division multiplexing (WDM) becomes research hotspot and develops rapidly[1–5]. Among all the available multi-wavelength generation schemes for WDM systems[6–13], including cascaded modulator, optoelectronic oscillator, and recirculating frequency shifter (RFS), RFS attracts more attention because of its wide band, low drive voltage, and tunable frequency spacing. A 113-tone optical frequency comb (OFC) has been generated by cascaded phase modulators and RFS loop[14]; however, there are several carriers generated at the same time because of the cascaded phase modulators, and these carriers and the ones generated in last loops will overlap with each other, which will affect the stability of the OFC. By using IQ modulator, single-sideband frequency shift can be achieved. RFS with single-sideband modulation can avoid the problem of overlapping, and a 50-tone wide-band OFC with high quality can be realized[11]. With double-RFS loop, OFC with 104 tones can be realized[15], and by using multi-carrier source input or multi-channel RFS loop[16,17], the number of tones can also be further increased. However, in these structures, because of the mismatch of multi-loop or multi-tone, system implementation will be very complex. So how to use single-RFS loop and single-sideband frequency shift to generate wide-band OFC is an attractive question. Even though the structure of the RFS loop is not very complex, every tone will travel around the loop dozens of times. The evolution of the noise characteristic in this process is a problem worth studying, especially phase noise, which has a significant impact on communication systems with complex modulation formats such as quadrature phase shift keying and orthogonal frequency division multiplexing.

In this letter, based on single-sideband modulation RFS structure, by optimizing the length and the gain of the loop, a 90-tone stable OFC with 4.26 dB peak-to-peak power fluctuation (PPPF) and tone-to-noise ratio (TNR) higher than 19.17 dB is realized. And it is analyzed and experimentally verified that the noise floor of the OFC accumulates linearly. Furthermore, in the process of frequency shifting, phase noise of radio frequency (RF) source and amplified spontaneous emission (ASE) noise of the erbium-doped fiber amplifiers (EDFAs) are introduced, which may influence the phase noise of the generated tones. Therefore, in order to analyze the phase noise of OFC generated by RFS, an experiment to measure the linewidth of the tones using delayed self-heterodyne interferometer (DSHI) technique is set up. The results show that the linewidth of the tones is nearly the same. So it infers that OFC based on RFS which has low-power fluctuation, high TNR and low linewidth is a good choice for broadband-optical communication systems.

The structure of an OFC generator based on RFS loop which consists of an IQ modulator, a band-pass filter (BPF), and an EDFA is shown in Fig. 1. The IQ modulator, which is made up of two Mach–Zehnder modulators (MZMs) and a phase shifter as shown in Fig. 2, is used to realize frequency shift by carrier-suppressed single-sideband modulation. The two MZMs are driven by RF signal with the same angular frequency ω_{RF} and amplitude A and $\pi/2$ phase difference. The bias points of both the MZMs and the phase difference between the MZMs are expected to set to their half-wave voltage V_{π} and $\pi/2$, respectively. The transfer function of the IQ modulation is shown as

$$T_{\mathrm{mod}} \approx -J_1\left(\frac{\pi A}{2V_{\pi}}\right)\exp[\mathrm{j}(\omega_{\mathrm{RF}}t + \varphi_{\mathrm{RF}}(t))], \tag{1}$$

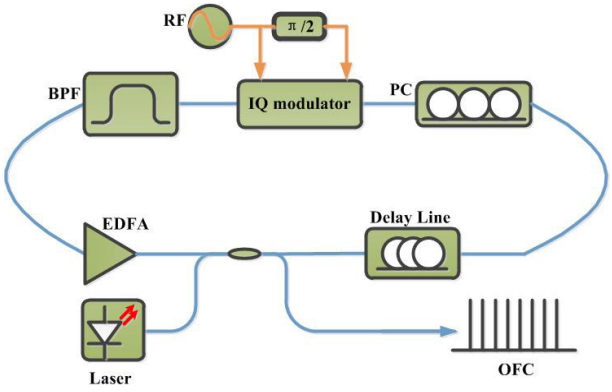

Fig. 1. Structure of an OFC generator based on RFS. PC, polarization controller.

where $\varphi_{RF}(t)$ represents the phase noise of the RF source, and the frequency shift is realized. The EDFA is used to fully compensate the loop loss, and the BPF is applied to limit the bandwidth of the OFC and filter out the out-of-band noise. So in setting up the stage of the OFC, every time it passes the RFS loop, all the tones shift ω_{RF}. And with the continuous injection of the laser, the OFC has one more tone. Only after the OFC fills the whole bandwidth of the BPF, an export stable OFC is achieved.

In our experiment, a delay line is added into the RFS loop to adjust the length of the loop and decrease the coherence of the tones in order to get a more stable OFC. The wavelength and the power of the laser are 1546 nm and 8 dBm, respectively. The frequency of the RF source is 10 GHz, and the bandwidth of the BPF is 0.9 THz. The signal-to-interference ratio and the suppression ratio of single sideband of IQ modulation are 28.86 and 29.35 dB, respectively, as shown in Fig. 3, and the power loss of the IQ modulator caused by insertion and frequency shifting is about 22dB. A 90-tone stable OFC is obtained as shown in Fig. 4. The worst TNR is 19.17 dB and the PPPF of the OFC is 4.26 dB. It is a wide-band flat OFC with high TNR.

As the OFC is expected to be applied in optical communication systems, besides bandwidth and PPPF, noise is also a significant influence factor on the transmission performance. So here we also analyze the noise feature of the OFC.

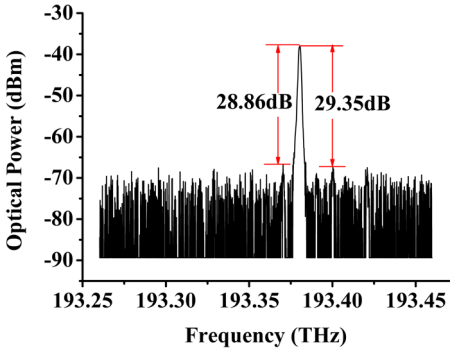

Fig. 3. Single-sideband modulation.

The transfer function of the RFS loop can be written as

$$T_{RFS} = \{\exp[j(\omega_{RF}t + \varphi_{RF}(t))] * f(t) + \text{noise}_{ASE}(t)\} \times \exp(j\varphi_{loop}(t)), \quad (2)$$

where $f(t)$ is the response function of the BPF and $\text{noise}_{ASE}(t)$ is the ASE noise introduced by EDFA; $\varphi_{loop}(t)$ represents the phase change caused by the loop jitter. The main source of the noise floor is the ASE noise. When the OFC passes EDFA, the wide-band ASE noise is introduced. Every time the OFC travels around the RFS loop, the noise floor shifts because of the IQ modulation, and new ASE noise adds onto the whole band. So the more times a tone travels around the RFS loop, the more ASE noise accumulates. That is to say, the noise floor increases linearly with the frequency shifting further from the frequency of the laser. When the power is measured in decibels, it looks like logarithmic function as shown in Fig. 4. A 50-tone, a 60-tone, a 70-tone, and an 80-tone OFCs are also generated and the noise floor of them is perfectly fit with logarithmic function as shown in Fig. 5.

Furthermore, the phase noise of the OFC is also studied. Noise in the loop includes phase noise of laser and RF source, ASE noise, carriers left by modulation and noise caused by loop jitter. As shown in Figs. 3 and 4, the power of carriers left by modulation and noise floor

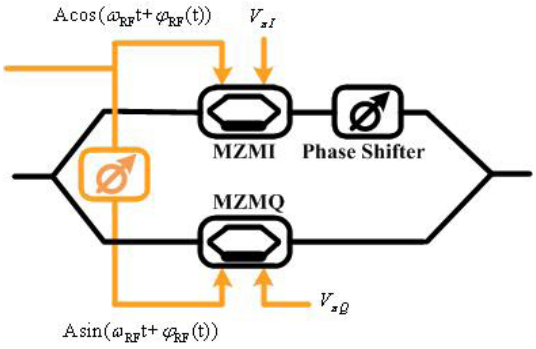

Fig. 2. Structure of the IQ modulator.

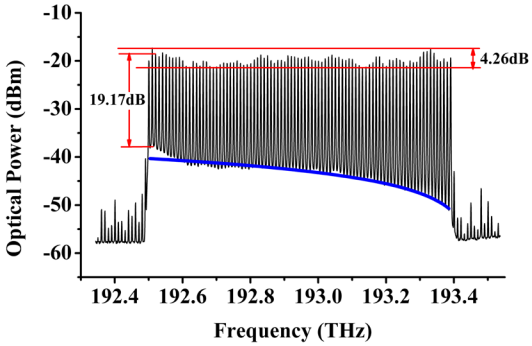

Fig. 4. Spectrum of the 90-tone OFC generated.

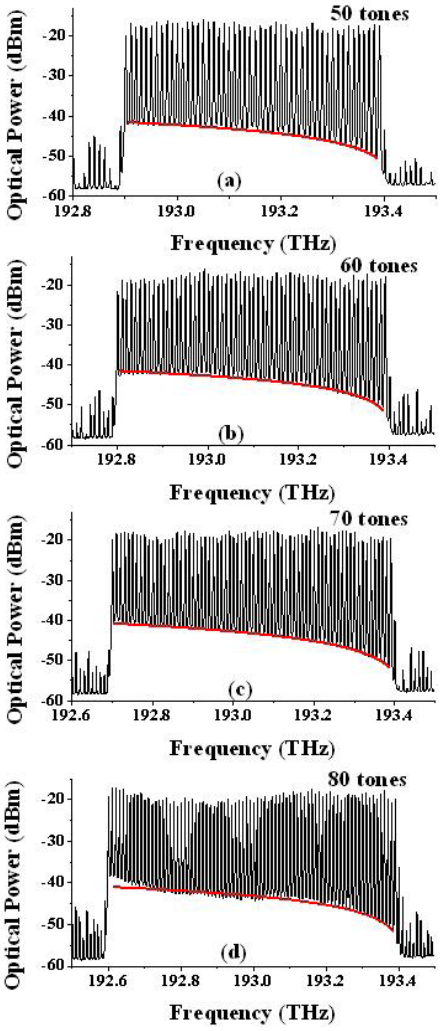

Fig. 5. Spectra of an OFC and noise floor fitting: (a) 50-tone, (b) 60-tone, (c) 70-tone, and (d) 80-tone OFCs.

are much lower than the power of the tones of OFC, and linewidth of RF source is much smaller than that of laser, but the tones travel around the loop dozens of times, and the noise accumulation may introduce more phase noise which will influence the performance of the communication systems.

In order to make sure the feather of the phase noise of the tones in OFC generated, an experiment to measure linewidth of the tones by using DSHI technique is accomplished as shown in Fig. 6(a). By using RFS, a 10 GHz-spaced OFC is generated as shown in Fig. 6(b). The waveshaper is a programmable filter. It is set as a BPF whose center frequency is aligned to the frequency of the tone to be measured, and the bandwidth is set as minimum value which is 10 GHz. After filtering, only this tone is left as shown in Fig. 6(c). Then the tone is divided into two parts by a 50:50 coupler, and one part injects into an acoustic optical modulator (AOM) to achieve a frequency shift of 27.12 MHz, and the other part passes 80 km single mode fiber (SMF). Then the two parts are put into a coupler and then injected into a balanced photoelectric detector (BPD) in order

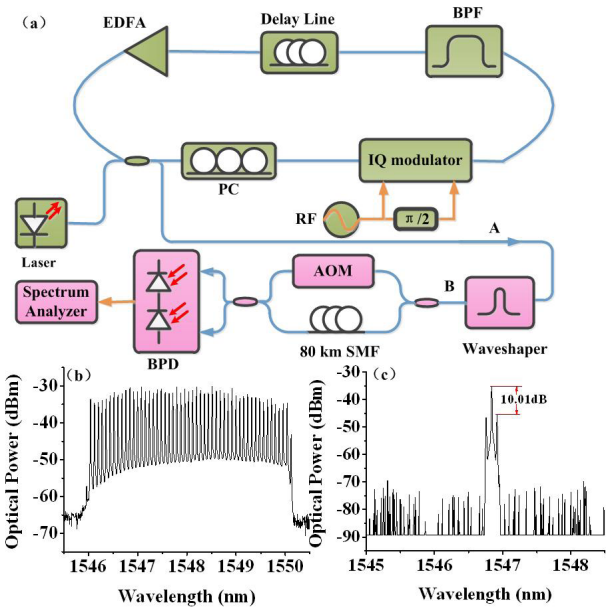

Fig. 6. (a) Structure diagram of the linewidth measurement experiment, (b) spectrum at point A, and (c) spectrum at point B.

to get the result of their beat frequency. The result is shown in the spectrum analyzer whose resolution is 1 kHz, black lines in Fig. 7, and is fit according to the Lorentz function, red line in Fig. 7. The full-width at half-maximum (FWHM) of the Lorentz function is two times that of the measured linewidth of the tone[18]. For every measured tone, six sets of data are collected, and the average FWHM of the data whose standard error of FWHM in fitting is less than 2 kHz is considered to be the linewidth of the tone. The linewidth of a tone is measured for every fifth tone and the result is shown in Fig. 8. The fluctuation range of the linewidth measured is 1.86 kHz.

An OFC with 12.5 GHz frequency interval is also generated and the linewidth of some tones is also measured. The spectrum of the OFC and the value of the linewidth measured are shown in Fig. 9. The fluctuation range of the linewidth measured is 3.36 kHz. It can be seen from the experimental results that the fluctuation

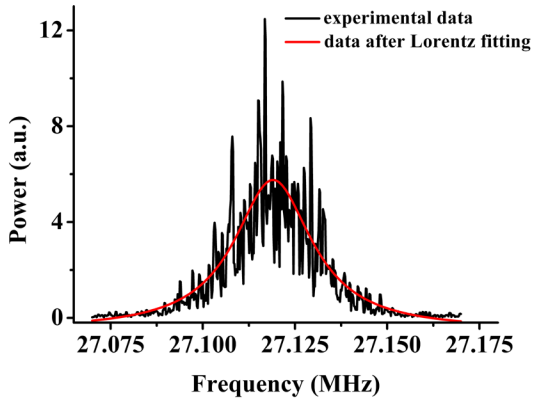

Fig. 7. Experimental data and fitting data.

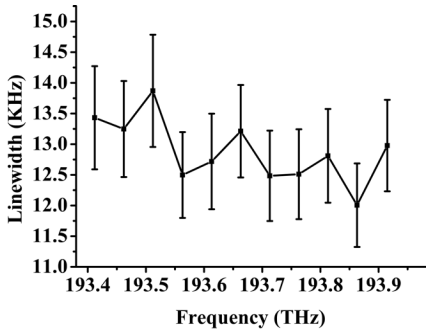

Fig. 8. Linewidth of tones.

range of the linewidth measured is very small, and it means that the linewidth of the tones does not increase with frequency shifting.

In conclusion, a 90-tone OFC with 10 GHz frequency interval is generated successfully by using carrier-suppressed single-sideband modulation RFS. The PPPF is 4.26 dB and the TNR is higher than 19.17 dB. Moreover, some analysis on the noise characteristic of the OFC based on RFS is also accomplished. The results show that the noise floor of the OFC accumulates linearly and the linewidth of the tones will not increase obviously with the frequency shifting. It indicates that RFS is able to generate OFC with broad bandwidth, good flatness, high TNR, and uniform linewidth for high-speed optical communication systems.

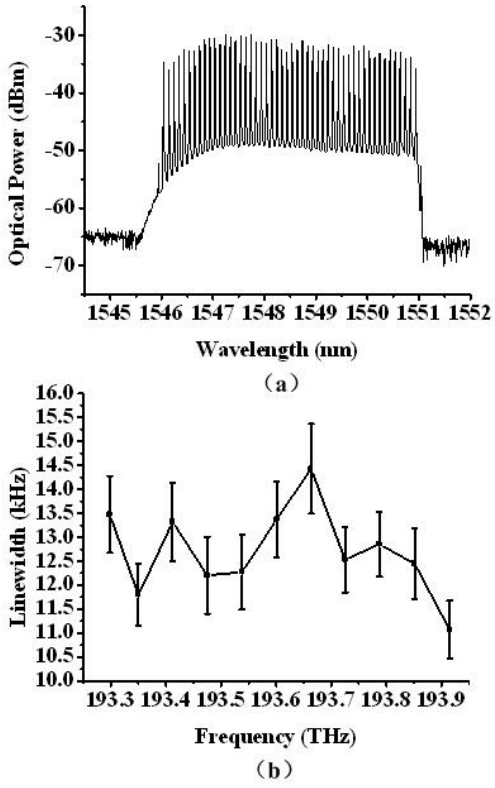

Fig. 9. (a) Spectrum of the OFC with 12.5 GHz frequency interval and (b) linewidth of the tones.

This work was supported by the National 973 Program of China (No. 2012CB315703), the National Natural Science Foundation of China (Nos. 61132004, 61335002, 61322113, and 61120106001), the Program for New Century Excellent Talents in University (No. NCET-10-0520), the Young top-notch Talent Program sponsored by Ministry of Organization, China, and the Tsinghua University Initiative Scientific Research Program.

References

1. Y. Ma, Q. Yang, Y. Tang, S. Chen, and W. Shieh, Opt. Express **17,** 9421 (2009).
2. J. Yu, Z. Dong, and N. Chi, Photon. Technol. Lett. IEEE **23,** 1061 (2011).
3. X. Liu, S. Chandrasekhar, B. Zhu, and D. W. Peckham, in *Proceedings of Optical Fiber Communication Conference* (2010).
4. X. Liu, D. M. Gill, S. Chandrasekhar, L. L. Buhl, M. Earnshaw, M. A. Cappuzzo, L. T. Gomez, Y. Chen, F. P. Klemens, E. C. Burrows, Y.-K. Chen, and R. W. Tkach, in *Proceedings of ECOC 2009* (2009).
5. H. Yu, H. Chen, M. Chen, and S. Xie, Chin. Opt. Lett. **11,** 100604 (2013).
6. T. Sakamoto, T. Kawanishi, and M. Izutsu, in *Proceedings of Lasers and Electro-Optics* (2006).
7. Y. Dou, H. Zhang, and M. Yao, Photon. Technol. Lett. IEEE **24,** 727 (2012).
8. R. Wu, V. R. Supradeepa, C. M. Long, D. E. Leaird, and A. M. Weiner, in *Proceedings of 2010 IEEE International Topical Meeting on Microwave Photonics* (2010).
9. M. Wang and J. Yao, IEEE Photon. Technol. Lett. **25,** 2035 (2013).
10. T. Kawanishi, T. Sakamoto, S. Shinada, and M. Izutsu, IEICE Electron. Express **1,** 217 (2004).
11. F. Tian, X. Zhang, J. Li, and L. Xi, J. Lightwave Technol. **29,** 1085 (2011).
12. S. Zou, Y. Wang, Y. Shao, J. Zhang, J. Yu, and N. Chi, Chin. Opt. Lett. **10,** 070605 (2012).
13. J. Yu, X. Li, J. Yu, and N. Chi, Chin. Opt. Lett. **11,** 110606 (2013).
14. J. Zhang, N. Chi, J. Yu, Y. Shao, J. Zhu, B. Huang, and L. Tao, Opt. Express **19,** 12891 (2011).
15. J. Zhang, J. Yu, N. Chi, Y. Shao, L. Tao, J. Zhu, and Y. Wang, J. Lightwave Technol. **30,** 3938 (2012).
16. J. Zhang, J. Yu, N. Chi, Y. Shao, L. Tao, Y. Wang, and X. Li, Photon. Technol. Lett. IEEE **24,** 1405 (2012).
17. J. Zhang, J. Yu, N. Chi, Z. Dong, X. Li, Y. Shao, and L. Tao, Opt. Lett. **37,** 4714 (2012).
18. T. Okoshi, K. Kikuchi, and A. Nakayama, Electron. Lett. **16,** 630 (1980).